Inorganic Chemistry

Article

pubs.acs.org/IC

Electronic Structures and Spin Density Distributions of BrO_2 and $(HO)_2BrO$ Radicals. Mechanisms for Avoidance of Hypervalency and for Spin Delocalization and Spin Polarization

Rainer Glaser* and Cory Camasta

Department of Chemistry, University of Missouri, Columbia, Missouri 65211, United States

Supporting Information

ABSTRACT: The results are reported of an ab initio study of bromine dioxide BrO_2, **1**, and of the T-shaped trans- and cis-dihydroxides **2** and **3** of dihydrogen bromate $(HO)_2BrO$. The thermochemistry has been explored of potential synthetic routes to $(HO)_2BrO$ involving water addition to BrO_2, hydroxyl addition to bromous acid HOBrO, **4**, protonation/reduction of bromic acid $HOBrO_2$, **5**, via tautomers **6**–**8** of protonated bromic acid, and by reduction/protonation of bromic acid via radical anion $[HOBrO_2]^-$, **9**. The potential energy surface analyses were performed at the MP2(full)/6-311G* level (or better) and with the consideration of aqueous solvation at the SMD(MP2(full)/6-311G*) level (or better), and higher-level energies were computed at levels up to QCISD(full,T)/6-311++G(2df,2pd)//MP2. The addition of RO radical to bromous acid or bromite esters and the reduction of protonated bromic acid or protonated bromate esters are promising leads for possible synthetic exploration. Spin density distributions and molecular electrostatic potentials were computed at the QCISD(full)/6-311G*//MP2(full)/6-311G* level to characterize the electronic structures of **1**–**3**. Both radicals employ maximally occupied (pseudo) π-systems to transfer electron density from bromine to the periphery. While the formation of the (3c-5e) π-system suffices to avoid hypervalency in **1**, the formation of the (4c-7e) π-system in **2** or **3** still leaves the bromine formally hypervalent and $(HO)_2BrO$ requires delocalization of bromine density into σ*-SMOs over the trans O–Br–O moiety. Molecular orbital theory is employed to describe the mechanisms for the avoidance of hypervalency and for spin delocalization and spin polarization. The (4c-7e) π-system in **2** is truly remarkable in that it contains *five* π-symmetric spin molecular orbitals (SMO) with unique shapes.

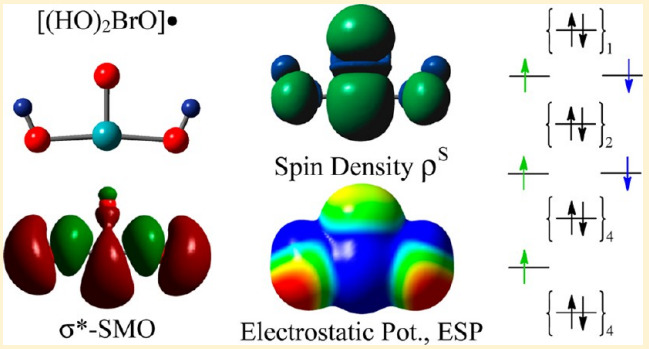

INTRODUCTION

In 1969, Musher originally defined a hypervalent molecule as a molecule with a central atom of group 15–18 in any of their valences other than their lowest stable chemical valence of 3, 2, 1, and 0, respectively.[1] Jensen[2] recently reviewed the origin of the term "hypervalency" and explained how the discussion of hypervalent molecules has revolved around the issue as to whether the 2-center-2-electron (2c-2e) bond or the octet rule is the more rigorous bonding principle. The Rundle–Pimentel model[3] invoked 3-center-4-electron (3c-4e) σ-bonds to describe formally hypervalent molecules; this model has been well supported by theoretical studies,[4−7] and it has become part of IUPAC's definition of hypervalency.[8] Qualitative descriptions of hypervalent molecules have been provided within the frameworks of molecular orbital (MO) theory[9b] and valence bond (VB) theory,[10−13] the role of d-orbitals has been clarified,[14,15] the term "hypercoordinate" has been discussed as an alternative to "hypervalent,"[16] and the concept of hypervalency continues to play an important role in discussions of descriptive inorganic chemistry.[17−19] While bromine oxoacids $HOBrO_n$ (n = 1, 2) and bromine dioxide BrO_2 are well-known hypervalent bromine compounds,[20] exciting developments have recently been made in the chemistry of λ^3-bromanes.[21−24]

Here we report the results of an ab initio study of bromine dioxide BrO_2, **1**, and of the isomers **2** and **3** of dihydrogen bromate $(HO)_2BrO$ (Scheme 1). The thermochemistry has been explored of four potential formations of $(HO)_2BrO$. First, dihydrogen bromate formally is the water adduct of BrO_2, and the reaction energy is reported for the addition reaction $BrO_2 + H_2O \rightarrow (HO)_2BrO$. Second, we studied the thermochemistry of hydroxyl addition to bromous acid HOBrO, **4**. Third, to explore the possibility of $(HO)_2BrO$ formation by protonation of bromic acid $HOBrO_2$, **5**, and subsequent reduction of protonated bromic acid, we determined the structures of isomers **6**–**8** resulting by protonation of bromic acid at the hydroxyl-O, at an oxo-O, or at bromine, respectively. Fourth, we determined the structure of radical anion $[HOBrO_2]^-$, **9**, the product of single-electron reduction of bromic acid, and the stability of its dative $HO^-\cdots BrO_2$ bond.

Received: May 13, 2013
Published: October 3, 2013

dx.doi.org/10.1021/ic4011967 | Inorg. Chem. 2013, 52, 11806–11820

Scheme 1. Nonpolar, Oxygen-Centered Radical Resonance Forms of $\lambda^3\sigma^2$-Bromine Dioxide BrO_2, 1, and of the trans- and cis-Isomers 2 and 3 of $\lambda^3\sigma^3$-Dihydrogen Bromate $(HO)_2BrO$[a]

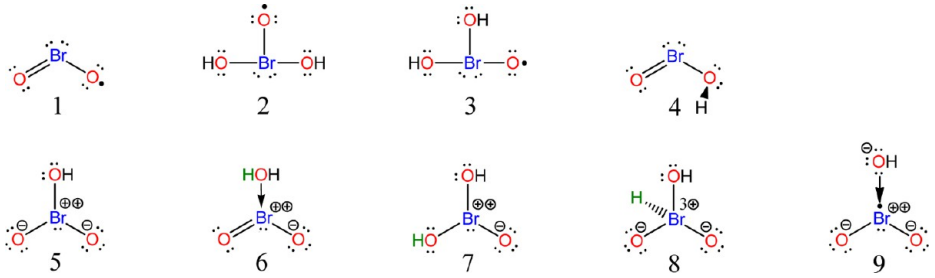

[a]The thermochemistry was studied of the addition of water to **1** and of the addition of hydroxyl to bromous acid, **4**. Bromic acid $HOBrO_2$ **5** and isomers **6**–**8** of protonated bromic acid were studied to explore the possible formations of **2** and **3** from **5** by protonation and reduction. The single-electron reduction of bromic acid to radical anion $[HOBrO_2]^-$ **9** also was studied.

Table 1. Relative and Reaction Energies Computed with the MP2 Structures[a,b,c]

parameter	ΔE	ΔH_0	ΔH_{298}	ΔG_{298}	$\Delta E'$	$\Delta G'$
2b vs **2a**	0.13	0.12	0.12	0.53	0.97	1.36
2c vs **2a**	0.39	0.19	0.32	0.42	−2.10	−2.07
2d vs **2a**	10.01	9.31	8.70	10.12	8.30	8.42
2e vs **2a**	5.33	4.71	4.08	5.13	2.12	1.92
3a vs **2a**	0.24	1.20	0.90	1.44	2.26	3.46
3b vs **2a**	0.71	1.75	1.49	1.96	2.44	3.69
3c vs **2a**	1.15	1.80	1.25	2.22	2.04	3.12
3d vs **2a**	2.52	3.03	2.47	3.48	2.94	3.90
3e vs **2a**	7.98	8.78	8.19	9.24	8.38	9.63
3c vs **3b**	0.44	0.05	−0.24	0.26	−0.40	−0.57
3d vs **3a**	2.28	1.83	1.58	2.04	0.68	0.44
3e vs **3b**	7.27	7.03	6.70	7.28	5.93	5.94
3c vs **2c**	0.76	1.61	0.93	1.80	4.15	5.19
1 + H_2O → **2a**	36.44	37.84	37.60	47.63	21.62	32.81
1 + H_2O → **2c**	36.83	38.02	37.92	48.05	19.52	30.74
4 + HO → **2a**	−2.88	−0.28	−0.56	9.06	−6.24	5.69
4 + HO → **2c**	−2.49	−0.09	−0.24	9.48	−8.34	3.62
6b vs **6a**	0.42	0.21	−0.20	0.64	0.59	0.81
6c vs **6a**	−1.39	−1.44	−1.56	−1.05	3.21	3.55
7a vs **7c**	1.08	1.03	1.01	1.06	0.96	0.94
7b vs **7c**	0.75	0.51	0.59	0.33	0.31	−0.12
7e vs **7c**	2.94	2.74	2.91	2.26	2.83	2.14
8b vs **8a**	8.17	7.58	7.29	7.80	7.43	7.06
7c vs **6a**	28.70	29.07	28.18	30.82	11.78	13.91
8a vs **6a**	107.64	107.31	106.10	109.35	93.67	95.38
5 + H_3O^+ → **6a** + H_2O	−28.37	−30.09	−29.15	−30.43	−14.99	−17.05
5 + H_3O^+ → **7c** + H_2O	0.33	−1.02	−0.96	0.39	−3.20	−3.14
EA(**2a**,**6a**)	150.52	151.39	151.92	150.41	181.16	181.04
EA(**2a**,**7c**)	179.22	180.45	180.10	181.23	192.94	194.96
EA(**9**,**5**)	47.63	49.58	49.09	50.57	45.72	48.66
HO^- + BrO_2 → **9**	−39.88	−38.15	−37.83	−29.68	−39.22	−29.02

[a]Relative energies in kcal/mol computed at the MP2(full)/6-311G* level. [b]Relative energies $\Delta E'$ in kcal/mol computed at the QCISD(full)/6-311G*//MP2(full)/6-311G* level. The $\Delta G'$ values are in kcal/mol and include MP2(full)/6-311G* thermochemical parameters; $\Delta G' = \Delta E' + (\Delta G - \Delta E)$. [c]Relative and reaction energies involving at least one anionic species are evaluated using the respective data computed at the levels MP2(full)/6-311++G** and QCISD(full)/6-311++G**//MP2(full)/6-311++G** level.

The present study focuses on the analysis of the electronic structure of $(HO)_2BrO$ and its comparison to the electronic structure of BrO_2. Both radicals are formally hypervalent and both employ maximally occupied π-systems to transfer electron density from bromine to the periphery. While the formation of the 3-center-5-electron (3c-5e) π-system suffices to avoid hypervalency in **1**, the formation of the 4-center-7-electron (4c-7e) π-system in **2** or **3** still leaves the bromine formally hypervalent, and $(HO)_2BrO$ requires delocalization of bromine density into σ^*-MOs over the HO−Br−OH moiety. Spin density distributions and molecular electrostatic potentials (ESPs) are reported to characterize the electronic structures of **1**–**3**. Molecular orbital theory is employed to describe the mechanisms for the avoidance of hypervalency and for spin delocalization and spin polarization. The (4c-7e) π-system in C_{2v}-**2c** is quite unusual in that it contains *five* π-symmetric spin molecular orbitals

dx.doi.org/10.1021/ic4011967 | *Inorg. Chem.* 2013, 52, 11806−11820

Table 2. Relative and Reaction Energies Computed with the SMD(MP2) Structures[a,b,c]

parameter	ΔE^{SMD}	ΔH_0^{SMD}	ΔH_{298}^{SMD}	ΔG_{298}^{SMD}	$\Delta E''$	$\Delta G''$
2c vs **2a**	2.38	1.39	0.89	2.11	−0.11	−0.38
1 + H_2O → **2a**	40.76	42.92	42.08	51.70	25.94	36.88
1 + H_2O → **2c**	43.14	44.31	42.97	53.81	25.84	36.50
4 + HO → **2a**	1.66	4.75	3.95	13.46	−1.70	10.10
4 + HO → **2c**	4.04	6.13	4.84	15.57	−1.82	9.72
6b vs **6a**	1.49	0.71	0.67	0.55	1.66	0.72
6c vs **6a**	0.60	−0.12	0.17	−0.42	5.20	4.18
7a vs **7c**	0.01	−0.06	−0.01	−0.16	−0.11	−0.28
7b vs **7c**	−0.77	−0.57	−0.72	−0.44	−1.22	−0.88
7e vs **7c**	1.59	1.96	1.86	2.08	1.48	1.96
7c vs **6a**	23.98	23.55	23.09	24.40	7.08	7.49
5 + H_3O^+ → **6a** + H_2O	7.87	5.76	6.77	6.82	21.25	20.20
5 + H_3O^+ → **7c** + H_2O	31.85	29.31	29.86	31.22	28.31	27.69
EA(**2a**,**6a**)	102.65	104.20	104.26	104.20	133.29	134.84
EA(**2a**,**7c**)	126.63	127.75	127.36	128.60	149.35	142.33
EA(**9**,**5**)	105.14	107.20	106.59	108.48	103.23	106.57
HO^- + BrO_2 → **9**	−5.03	−3.50	−3.38	4.58	−4.37	5.24

[a]Relative energies in kcal/mol computed at the SMD(MP2(full)/6-311G*) level. [b]Relative energies $\Delta E''$ in kcal/mol computed at the SMD(MP2(full)/6-311G*) level and accounting for the QCI correction computed at the QCISD(full)/6-311G*//MP2(full)/6-311G**level. $\Delta E'' = \Delta E' + (\Delta E^{SMD} - \Delta E)$ and $\Delta G'' = \Delta E'' + (\Delta G^{SMD} - \Delta E^{SMD})$. [c]Relative and reaction energies involving at least one anionic species are evaluated using the respective data computed at the levels SMD(MP2(full)/6-311++G**) and employing the QCI corrections computed at the QCISD(full)/6-311++G**//MP2(full)/6-311++G** level.

Table 3. Relative and Reaction Energies Computed with the Extended Basis Set 6-311++G(2df,2pd) at the QCISD and QCISD(T) Levels for the MP2 Structures[a,b,c]

	Q2 Level QCISD/6-311++G(2df,2pd)			Q3 Level QCISD(T)/6-311++G(2df,2pd)		
parameter	ΔE^{Q2}	ΔE^{Q2S}	ΔG^{Q2S}	ΔE^{Q3}	ΔE^{Q3S}	ΔG^{Q3S}
2c vs **2a**	−4.49	−2.50	−2.46[d]	−4.48	−2.49	−2.46[d]
1 + H_2O → **2a**	25.55	29.87	40.81	28.04	32.36	43.30
1 + H_2O → **2c**	21.06	27.37	38.60[d]	23.55	29.87	41.09[d]
4 + HO → **2a**	−8.82	−4.28	7.52	−10.21	−5.68	6.13
4 + HO → **2c**	−13.30	−6.78	5.19[d]	−14.69	−8.17	3.80[d]
7a vs **7c**	−0.26	−1.33	−1.50	0.02	−1.06	−1.23
7b vs **7c**	−0.49	−2.02	−1.68	−0.20	−1.73	−1.39
7a vs **6a**	1.73	−4.06	−3.81	7.70	1.90	2.15
7b vs **6a**	1.50	−4.75	−3.99	7.48	1.23	1.99
7c vs **6a**	1.99	−2.73	−2.31	7.68	2.96	3.38
5 + H_3O^+ → **6a** + H_2O	−10.83	25.41	24.36	−16.19	20.04	19.00
5 + H_3O^+ → **7c** + H_2O	−8.84	22.68	22.05	−8.51	23.00	22.38
EA(**2a**,**6a**)	191.72	143.85	145.40	182.83	134.97	136.52
EA(**2a**,**7c**)	193.71	141.12	143.10	190.51	137.92	139.90
EA(**9**,**5**)	36.75	94.26	97.60	37.78	95.29	98.63
HO^- + BrO_2 → **9**	−38.40	−3.55	6.06	−40.24	−5.39	4.22

[a]Relative energies ΔE^{Qn} in kcal/mol and based on MP2(full)/6-311G* structures (neutral molecules and cations). [b]Relative energies ΔE^{QnS} in kcal/mol computed at the Q2 and Q3 levels and accounting for solvation corrections computed at the SMD(MP2) level. $\Delta E^{QnS} = \Delta E^{Qn} + (\Delta E^{SMD} - \Delta E)$ and $\Delta G^{QnS} = \Delta E^{QnS} + (\Delta G^{SMD} - \Delta E^{SMD}) = \Delta E^{Qn} + (\Delta G^{SMD} - \Delta E)$. [c]Relative and reaction energies involving at least one anionic species are evaluated using the respective data computed at the levels SMD(MP2(full)/6-311++G**) and employing the QCI corrections computed with the MP2(full)/6-311++G** structures. [d]Computed via $\Delta G^{QnS} = \Delta E^{QnS} + (\Delta G - \Delta E)$.

(SMOs) with unique shapes, and it is shown how this feature contributes to the spin polarization of the Br−O bond.

■ COMPUTATIONAL AND THEORETICAL METHODS

Potential energy surface (PES) analyses[25] were performed with second-order Møller−Plesset perturbation theory (MP2)[26,27] in conjunction with the 6-311G* basis set,[28] MP2(full)/6-311G*, to locate and characterize minima and transition state structures. Single point energies were computed for all of the MP2 structures using the QCISD(full) method[29,30] and the same basis set; QCISD(full)/6-311G*//MP2-(full)/6-311G* (:= Q1 for short). For selected systems, single point energies also were computed with the QCISD(full) and QCISD(full,T) methods and the extended basis set[31] 6-311++G(2df,2dp) for the MP2(full)/6-311G* structures; QCISD(full)/6-311++G(2df,2pd)//MP2(full)/6-311G* (:= Q2 for short) and QCISD(full,T)/6-311++G(2df,2pd)//MP2(full)/6-311G* (:= Q3 for short). Unrestricted wave functions were employed for all radicals, all electrons were included in the active space in all MP2 and QCISD computations, and sets of five orthogonal d-functions and seven orthogonal f-functions were employed in all computations.

The protonation of bromic acid requires the consideration of solvation effects, and we studied all four potential formation reactions with the solvation model density (SMD) method.[32,33] The SMD

dx.doi.org/10.1021/ic4011967 | Inorg. Chem. 2013, 52, 11806−11820

method is a density-based, self-consistent reaction field theory of bulk electrostatics (SCRF) which accounts for long-range electrostatic polarization (bulk solvent) and also for short-range effects associated with cavitation, dispersion, and solvent structural effects (CDS). We employed the SMD method at the MP2(full)/6-311G* level, and this SMD(MP2(full)/6-311G*) level is referred to as SMD(MP2) for brevity.

The study of radical anion **9** requires the augmentation of the basis set with diffuse functions and the structure of **9** was optimized at the theoretical levels MP2(full)/6-311++G** and SMD(MP2(full)/6-311++G**). For **9**, all QCISD energies are based on the MP2(full)/6-311++G** structure and Q1 refers to the level QCISD(full)/6-311++G**//MP2(full)/6-311++G**. The evaluations of the electron affinity of bromic acid **5** and of the addition of hydroxide to bromine dioxide **1** require that all species are computed with the same basis set and, hence, we also computed hydroxide and the neutral species **1** and **5** at these same levels.

Computations were performed with Gaussian09[34] in conjunction with Gaussview 5,[35] on an SGI Altix BX2 SMP system and a Dell EM64T cluster system.

Total energies (E_{tot}), vibrational zero point energies (*VZPE*), thermal energies (*TE*), molecular entropies (*S*), and the two lowest vibrational frequencies ν_1 and ν_2 computed at the MP2 and SMD(MP2) levels are given in Supporting Information, Tables S1 and S2, respectively. The energies computed at the three QCISD levels Q1−Q3 are listed in the last three column of Supporting Information, Table S1. In Tables 1 and 2 are listed the relative and reaction energies computed at the MP2 level (ΔE, ΔH_0, ΔH_{298}, ΔG_{298}) and at the SMD(MP2) level (SMD superscript). Four thermodynamic values are provided for each parameter, and these are ΔE, $\Delta H_0 = \Delta E + \Delta VZPE$, $\Delta H_{298} = \Delta E + \Delta TE + \Delta(pV)$, and $\Delta G_{298} = \Delta H_{298} - 298.15 \cdot \Delta S$. We are primarily interested in condensed-phase chemistry, and $\Delta(pV)$ is assumed to be negligible. For reactions of ideal gases at room temperature, $\Delta(pV)$ is $\Delta n \cdot 0.593$ kcal/mol. The values $\Delta E'$ are based on the Q1 energies and $\Delta G' = \Delta E' + (\Delta G - \Delta E)$. The energies $\Delta E''$ also are based on the Q1 energies, but these values also include a correction for the solvent effects computed at the SMD(MP2); $\Delta E'' = \Delta E' + (\Delta E^{SMD} - \Delta E)$ and $\Delta G'' = \Delta E'' + (\Delta G^{SMD} - \Delta E^{SMD})$. The best data are summarized in Table 3, where we report ΔE^{Qn}, ΔE^{QnS} and ΔG^{QnS} values that are based on the Q2 and Q3 energies and account for solvation effects on energies computed at the SMD(MP2) level and also for the thermochemical properties computed at the SMD(MP2) level; $\Delta E^{QnS} = \Delta E^{Qn} + (\Delta E^{SMD} - \Delta E)$ and $\Delta G^{QnS} = \Delta E^{QnS} + (\Delta G^{SMD} - \Delta E^{SMD})$.

Electronic structures were characterized by inspection of the molecular ESPs[36] and by analyses of spin density distributions.[37] ESPs and spin densities were computed with the QCI densities determined at the QCISD(full)/6-311G*//MP2(full)/6-311G* level.[38−40]

RESULTS AND DISCUSSION

Bromine Dioxide, BrO_2. Bromine dioxide has been prepared by symproportionation of bromic acid and bromous acid in aqueous and organic solution[41,42] and also by irradiation of crystals of bromates.[43,44] The MP2/6-311G* structure of BrO_2 is C_{2v}-symmetric with Br−O bonds of 1.657 Å and a bonding angle $\angle$(O−Br−O) = 117.4°, and it agrees well with previous theoretical studies[45,46] and with the experimental microwave structure (1.649 Å, 114.44°).[47] BrO_2 has been well characterized spectroscopically,[47−50] and its low-lying electronic states also have been studied (doublet and quartet).[51]

The electronic structure of BrO_2 is readily understood[48,52] as a (3c-5e) π-system with configuration $(\pi_1)^2(\pi_2)^2(\pi_3)^1$ and the three π-MOs are shown schematically in Scheme 2. This (3c-5e) π-system is a "maximally occupied π-system" because $2n - 1$ electrons occupy a π-system spanned by n p-AOs and consisting of n π-MOs or $2n$ π-SMOs. A fully occupied π-system (i.e., $2n$ electrons in an n-center π-system) always is antibonding because the destabilization of an antibonding MO is larger in magnitude than the stabilization of a bonding MO.[9c] Hence, we use the term "maximally occupied π-system" to describe a π-system that contains as many electrons as possible while remaining overall bonding.

Scheme 2. Schematic Representations of the (3c-5e) π-System of BrO_2, 1[a]

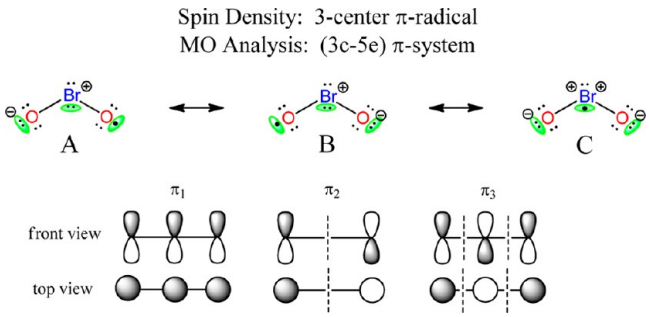

[a]The 5 electrons involved in the 3-center π-system are highlighted by green coloration in the Lewis structures.

For radicals, it is not strictly correct to talk about doubly occupied MOs because spin polarization causes the electrons in each "electron pair" to occupy slightly different α-spin molecular orbitals (ASMO) and β-spin molecular orbitals (BSMO) in unrestricted Hartree−Fock theory (UHF), and these UHF spin molecular orbitals are shown in Figure 1. Conversely, the

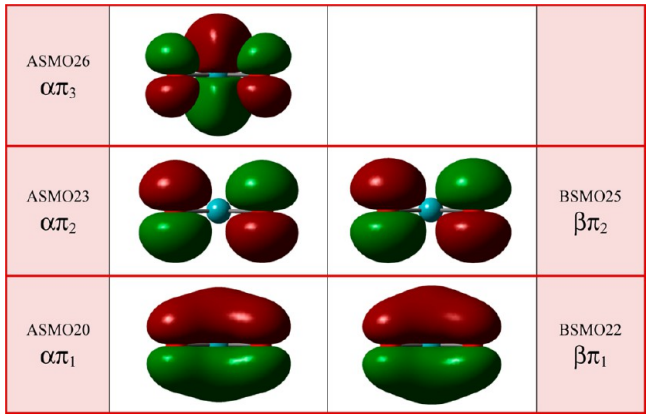

Figure 1. Electronic structure of BrO_2 radical, **1**. The π-MOs with α-spin (ASMO) and β-spin (BSMO) are shown.

preference for different α- and β-spin molecular orbitals may cause radicals to appear in singlet species. Many 1,3-dipoles,[53] including ozone, are well-known to prefer different α- and β-spin molecular orbitals to realize singlet diradical electronic structures. However, in most radicals, including BrO_2, there are pairs of α- and β-spin molecular orbitals which are shape-matched to a high degree and in such cases it makes sense to talk about near-perfectly paired electrons. In BrO_2, ASMO20 and BSMO22 describe the two electrons in the bonding π_1-MO, ASMO23 and BSMO25 describe the two electrons in the nonbonding π_2-MO, and ASMO26, the α-HOMO, describes the unpaired electron in the antibonding π_3-MO.

The spin density distribution of BrO_2 is shown in Figure 2 (top row) where regions of α- and β-spin density are shown in green and blue, respectively. The spin density distribution is fully consistent with expectations based on inspection of the α-HOMO and centers of α-spin density occur in p-shaped regions

dx.doi.org/10.1021/ic4011967 | Inorg. Chem. 2013, 52, 11806−11820

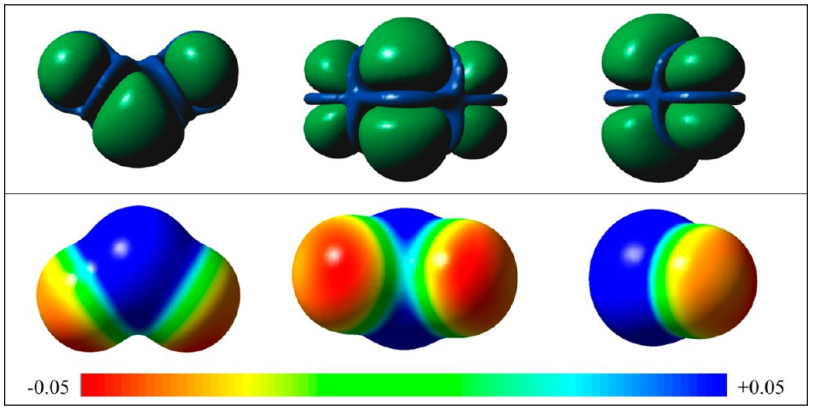

Figure 2. Electronic structure of BrO_2 radical, **1**. In the top row, the QCI//MP2 spin density distribution is shown as viewed from top, front (proximate Br), and side. Green and blue colors represent α- and β-spin density, respectively. In the bottom row, the QCI//MP2 ESP is shown surfaced mapped from −0.05 (red) to +0.05 au (blue) on the total electron density (ρ = 0.004 e·Å^{-3}) as viewed from top, back, and side.

Scheme 3. Conformations Considered for Trans- and Cis-Isomers 2 and 3 of $(HO)_2BrO$ Radical[a]

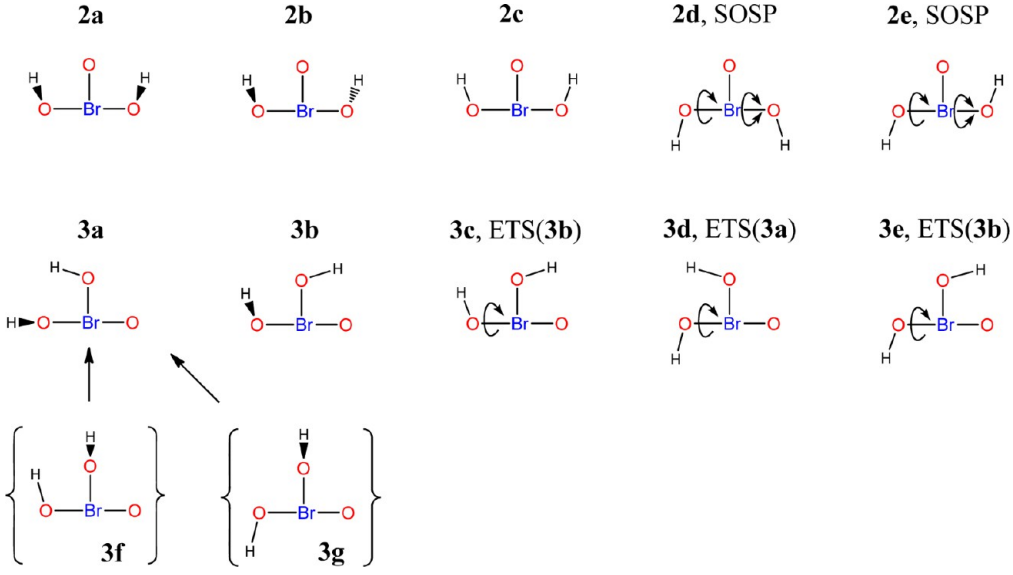

[a]All structures of $(HO)_2BrO$ radical are T-shaped.

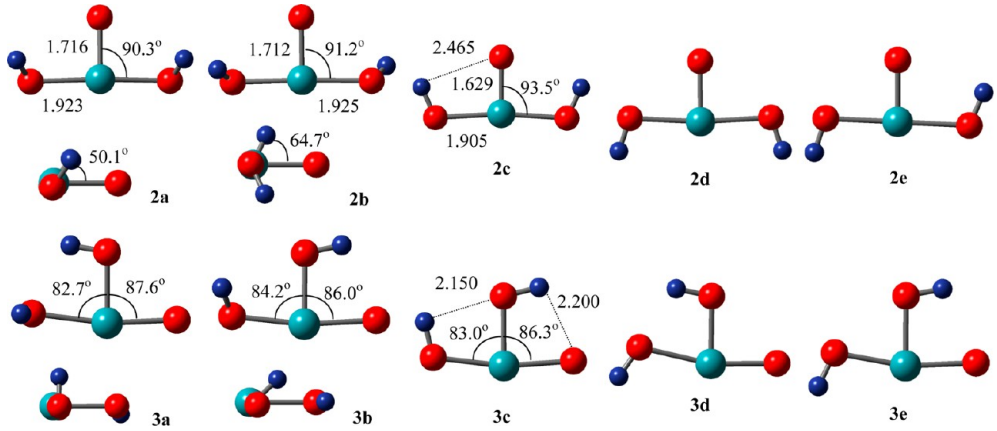

Figure 3. Stationary structures of isomers **2** and **3** of $(HO)_2BrO$ radical.

centered at all three atoms. Centers of α-spin density tend to spin-polarize the electron density of "paired" electrons in such a way as to further enhance the α-spin density at those centers while regions of β-spin density appear elsewhere in the molecule.[54−57] In BrO_2, regions of β-spin density appear in the node planes of the HOMO (blue in Figure 2).

The nonpolar resonance form of BrO_2 can be constructed as a π-radical with a (3c-5e) π-system. The essential feature that

dx.doi.org/10.1021/ic4011967 | Inorg. Chem. 2013, 52, 11806−11820

Table 4. Optimized Structures of Dihydrogen Bromate $(HO)_2BrO$[a]

parameter	2a, C_s	2b, C_2	2c, C_{2v}	2d, C_{2v}	2e, C_s	3a, C_1	3b, C_1	3c, C_s	3d, C_s	3e, C_s
Br−O	1.716	1.712	1.629	1.680	1.664	1.806	1.864	1.846	1.788	1.849
Br−OH	1.923	1.925	1.905	1.958	1.934	1.956	1.876	1.888	1.977	1.891
					1.930	1.837	1.840	1.845	1.819	1.817
HB(OH···O)	2.706	2.777	2.465		2.475	2.028	2.135	2.150	1.859	2.113
	2.706	2.777	2.465				2.433	2.200		
HO−Br−O	90.3	91.2	93.5	86.9	87.3	87.6	86.0	86.3	88.8	87.1
					92.8					
HO−Br−OH	173.7	177.5	173.0	173.7	179.9	82.7	84.2	83.0	77.7	80.2
H−O−Br	110.5	110.0	111.3	105.6	105.8	99.6	102.9	103.6	101.0	105.9
					110.9	109.4	110.1	110.2	112.4	101.3
H−O−Br−O	50.1	64.7	0.0	180.0	180.	90.1	45.2	0.0	180.0	0.0
					0.	165.7	3.1	0.0	180.0	180.
HO−Br−O−OH	174.2	180.0	180.	180.	180.	8.1	13.6	0.0	0.0	0.0
HO−Br−OH−O						178.6	177.6	180.0	180.0	180.0

[a]MP2(full)/6-311G* structures; bond lengths in Å, angles and dihedrals in degrees.

allows bromine in BrO_2 to avoid hypervalency is the access to the polar resonance forms **A**−**C**, and this access is directly connected to the formation of the (3c-5e) π-system. In the Lewis structures **A**−**C**, the (3c-5e) π-system involves the unpaired electron and one lone pair at each of the other atoms. The (3c-5e) π-system effectively removes at least one electron from bromine (**A** and **B** in Scheme 2), and the huge amount of spin density at bromine shows that Lewis structure **C** also plays a very important role and further increases the Br−O bond polarity. We computed the ESP of the QCI density of BrO_2 on surfaces defined by the total electron density, and the resulting surface maps show bromine to be highly electron-deficient (Figure 2).

Structures of Dihydrogen Bromate, $(HO)_2BrO$ Radical. The two hydroxyl groups are trans with regard to each other in isomer **2** while they are cis in isomer **3**. We located 10 structures, all are T-shaped (Scheme 3, Figure 3), and their structural parameters are collected in Table 4.

We first optimized the structures **2a** and **2b**, and their dihedral angles ∠(H−O−Br−O) are *not* close to zero. To assess the energy required for planarization, **2c** was optimized in C_{2v} symmetry with the expectation that **2c** would correspond to a second-order saddle point (SOSP) on the PES. Yet, at the level of optimization **2c** corresponds to an additional minimum, and **2a**−**2c** are within less than 1 kcal/mol (Table 1). We then optimized **2d** and **2e** and find that these structures do correspond to SOSPs, and both are considerably less stable than **2a**−**2c** (Table 1). The imaginary modes of **2d** and **2e** correspond to in-phase and out-of-phase rotations about the two HO−Br bonds as indicated by the curved arrows in Scheme 3.

In the cis-isomers **3a** and **3b**, only one of the two hydroxyl-H atoms is almost in the best plane of BrO_3. We optimized the planar structures **3c**−**3e** and find that they are transition state structures for enantiomerization, and their transition state vectors are indicated by the curved arrows in Scheme 3. For example, **3d** is the transition state structure for the enantiomerization of **3a**, ETS(**3a**), where ETS stands for "enantiomerization transition state." We searched for structures of types **3f** and **3g** and those searches returned to **3a** and **3b**, respectively.

One might have expected that structures with two intramolecular H-bonds would be best (i.e., **2a**−**2c**, **3b** and **3c**, dashed lines indicate H-bonding in Figure 3). The QCISD level computations are especially beneficial for the planar structures **2c**−**2e** and **3c**−**3e** (Table 1). The main result of the QCISD//MP2 computations is the insight that structures **2c** and **3c** featuring two intramolecular and in-plane H-bonds are slightly preferred. The analysis of the spin density distributions and ESPs of **2a**−**2c** and **3a**−**3c** will show that the electronic structures are very similar and common across the conformers. The thermochemistry clearly favors **2** over **3**, and the preference for **2** is more pronounced at the QCISD//MP2 level (Table 1).

We also optimized **2a** and **2c** at the SMD(MP2) level (Table 2) and determined their energies at the higher QCISD levels Q2 and Q3 (Table 3). Solvation effects provide a small advantage for **2a** over **2c**, while the preference for the planar structure **2c** over **2a** increases at the higher QCISD levels. These results show that the structure of radical **2** is rather flexible because a wide range of conformations about the two HO−Br bonds is readily accessible. We will consider both **2a** and **2c** in the discussion of possible formations of dihydrogen bromate below.

$(HO)_2BrO$ Radical Formation. The thermochemistry has been explored of four potential formation reactions of $(HO)_2BrO$ from the substrates bromine dioxide (water addition), bromous acid (hydroxylation), and bromic acid ($+H^+/+e^-$; $+e^-/+H^+$).

(a). Water Addition to Bromine Dioxide. The addition reaction $BrO_2 + H_2O \rightarrow (HO)_2BrO$ is endothermic by at least 20 kcal/mol in gas phase, it is significantly more endothermic in solution, and entropy makes the water addition even more unlikely (Tables 1−3). Hence, it is clear that $(HO)_2BrO$ will not be accessible by water addition to BrO_2.

(b). Hydroxyl Addition to Bromous Acid. $(HO)_2BrO$ might be accessible by addition of hydroxyl radical to bromous acid **4**, and we studied the reaction **4** + $HO^\bullet$ → **2a**/**2c**. The reaction energy of the addition reaction significantly depends on the quality of the correlation treatment. The addition is only slightly exothermic at the MP2 level of optimization $\Delta E = -2.9$ kcal/mol (Table 1) and at the highest QCI level the exothermicity increases to $\Delta E^{Q3} = -14.7$ kcal/mol (Table 3). The free enthalpy of hydroxyl addition is about 12 kcal/mol higher than the reaction energy (Table 1), and the hydroxyl addition in the gas phase is predicted to be almost thermoneutral on the ΔG surface. The SMD(MP2) results indicate that aqueous solvation causes a modest increase of the reaction energy of the addition, that the free enthalpy of the hydroxyl addition is about 10 kcal/mol higher than the reaction energy, and that the addition is endergonic by about 4−6 kcal/mol (Table 3).

(c). Protonation of Bromic Acid and Subsequent Reduction: Structures of Protonated Bromic Acid. The one-electron

dx.doi.org/10.1021/ic4011967 | Inorg. Chem. 2013, 52, 11806−11820

Scheme 4. Conformations Considered for Isomers 6−8 of $(HO)_2BrO$ Cation[a]

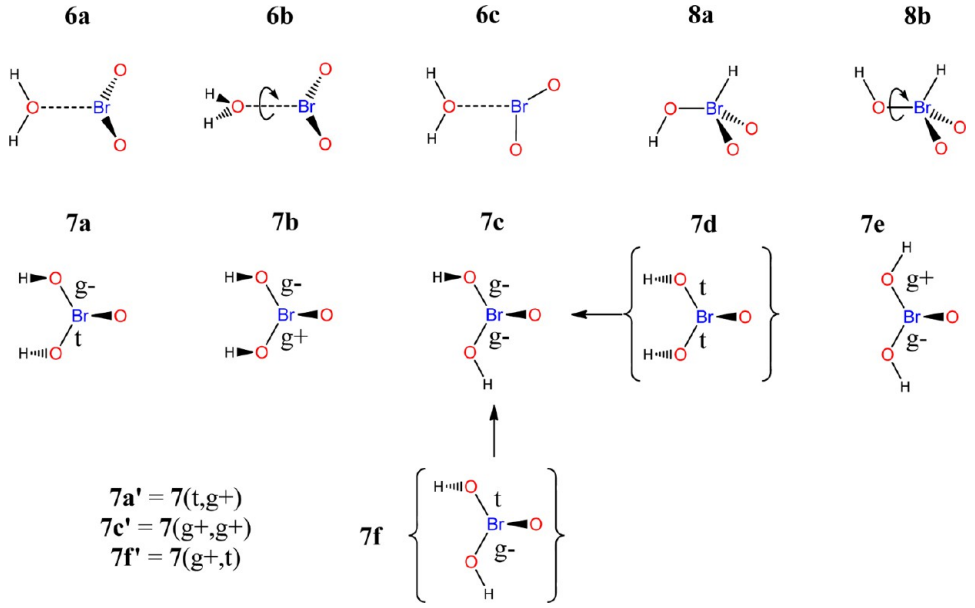

[a]For 7, the labels t, g+, and g− denote trans and gauche conformation about the HO−Br bonds.

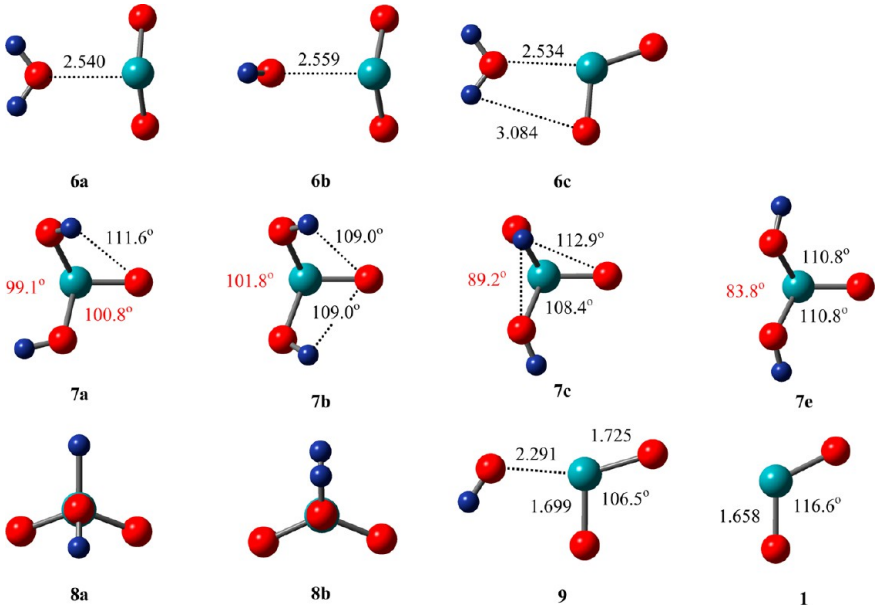

Figure 4. Stationary structures of isomers **6**−**8** of protonated $HOBrO_2$. Isomers **6**−**8** result by protonation of bromic acid at the hydroxyl-O, at an oxo-O, or at bromine, respectively. Stationary structure of bromic acid radical anion **9** and of BrO_2 computed at the MP2(full)/6-311++G** level.

reduction of O-protonated bromic acid,[58] $[(HO)_2BrO]^+$, presents a thermodynamically possible path for the formation of $(HO)_2BrO$ radical, and its synthetic accessibility depends on the relative stabilities of the isomers of protonated bromic acid and relative acidities of $[(HO)_2BrO]^+$ and H_3O^+.

We considered the three isomers **6**−**8** in the conformations shown in Scheme 4. Isomers **6**−**8** formally are the products of protonation of bromic acid at the hydroxyl-O, at an oxo-O, or at bromine, respectively. The structures of stationary structures are shown in Figure 4 and Cartesian coordinates of all structures are provided in the Supporting Information. Protonation at Br was considered merely for completeness, isomer **8** is clearly not competitive (Table 1), and the discussion will focus on the relevant isomers **6** and **7**.

Protonation of bromic acid at the hydroxyl-O results in structure **6a**, a hydrate of BrO_2 cation with a long $H_2O\cdots BrO_2$ bond, and the rotation about the $H_2O\cdots BrO_2$ bond via transition state structure **6b** is very facile (Figure 4, Table 1). Structures **6a** and **6b** can be seen as the result of dative bonding of a water lone pair and the π^3-LUMO of BrO_2 cation. Further exploration of the MP2(full)/6-311G* PES of **6** led to the unexpected discovery of an additional minimum **6c** which is slightly *more* stable than **6a** on the MP2 PES. Structure **6c** also is a hydrate of the BrO_2 cation, but **6c** is planar and the dative bonding of water involves a σ-LUMO of BrO_2 cation. Solvation effects are especially important for cations, and the study of **6a**−**6c** at the SMD(MP2) level again places **6c** very close to **6a** (Table 2). With the more complete treatment of electron correlation at the QCISD(full)/

dx.doi.org/10.1021/ic4011967 | *Inorg. Chem.* 2013, 52, 11806−11820

6-311G* level, the preference for **6a** over **6c** becomes more pronounced ($\Delta G' = 3.6$ kcal/mol; $\Delta G'' = 4.2$ kcal/mol).

The conformational space of isomer **7** can be discussed with the assumption of 3-fold barriers about both HO−Br bonds. With regard to the unique oxo-O, the hydroxyl-H can be in the trans position (t, ∠(H−O−Br−O) ≈ 180°) or in one of two gauche positions (g+, ∠(H−O−Br−O) ≈ +60°; (g−, ∠(H−O−Br−O) ≈ −60°). There are three pairs of enantiomers among the nine possible combinations, six conformations **7a**−**7f** were considered as initial structures, and the four stationary structures **7a**−**7c** and **7e** were located (Figure 4). All attempts to locate structures of type **7d** and **7f** led to **7c**.

The structures of the minima of **7** all are pyramidal, and a brief analysis of their ∠(O−Br−O) angles is instructive. The angles are included in Figure 4, the values that differ markedly from about 110° are highlighted in red, and it can be seen that the ∠(O−Br−O) angle becomes as low as 89° (**7c**) or even 84° (**7e**)! The polar resonance form shown for **7** in Scheme 1 contains just one lone pair at bromine, and this resonance form would predict a more or less tetrahedral structure; Bent's rule would suggest a reduction of the bond angles.[59] However, the actual lone pair density at Br is increased because of 2-fold O→Br π-backbonding to reduce the BO bond polarity in **7**. The analysis of **7e** is advantageous because of its symmetry, while it is representative of all minima of **7**, and the illustrations in Figure 5 show that MO30 and HOMO31 of **7e** are antibonding in the (BrO)-region. Single-electron reduction of **7** populates LUMO32 (vide infra), and this MO also is shown in Figure 5.

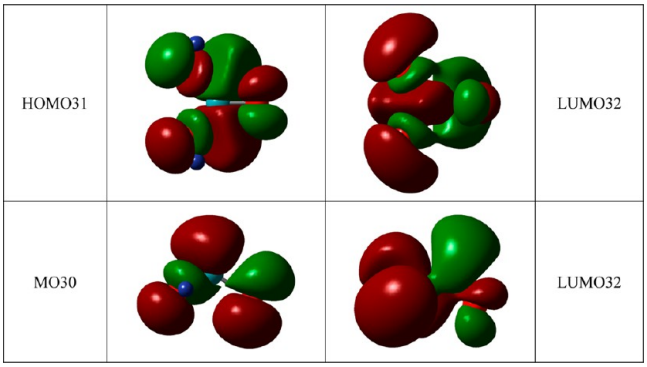

Figure 5. Molecular orbitals of protonated bromic acid isomer **7e**. In the images shown in the top row, the molecule's C_s-plane is perpendicular to the paper plane and horizontal. In the images shown in the bottom row, the molecule's C_s-plane coincides with the paper plane. MO30 and HOMO31 are antibonding π-type MOs in the (BrO)-region. Single-electron reduction of **7e** populates the LUMO32.

The isomers **7b** and **7c** both allow for two weak intramolecular H-bonding contacts (dashed in Figure 4), and they are slightly more stable that **7a** and **7e**; all of the minima **7a**−**7c** and **7e** are within 3 kcal/mol at the MP2 and QCISD//MP2 levels (Table 1). The SMD(MP2) level provides an advantage to isomers with hydrogen-bond donors and acceptors which are more available to interact with solvent water, and it make sense that **7a** becomes competitive with **7c** at the SMD(MP2) level. At the SMD(MP2) level, **7b** also becomes markedly favored over **7c**.

The relative stabilities of isomers **6** and **7** are consequential. Whereas the single-electron reduction of isomer **6** leads directly to BrO_2 radical, the reduction of **7** would lead to $(HO)_2BrO$ radical. We find a very strong preference of $\Delta E = 28.7$ kcal/mol for **6a** over **7c** at the MP2 level. The isomer preference for **6a** over **7c** is reduced somewhat to $\Delta E^{SMD} = 24.0$ kcal/mol when accounting for solvation effects at the SMD(MP2) level. However, the computations at the QCISD/MP2 level make a really dramatic difference in that **7** benefits *much more* than **6** from the improved electron correlation treatment: $\Delta E' = 11.8$ kcal/mol and $\Delta E'' = 7.1$ kcal/mol. This dramatic electron correlation effect on the relative stabilities of isomers **6** and **7** compelled us to compute the QCISD and QCISD(T) data with the extended basis set 6-311++G(2df,2pd), and we computed the relative energies of **6a** with respect to all three isomers **7a**−**7c** (Table 3). At the very least, these data confirm that **7** *can compete with* **6**. One could employ still higher levels of theory to further bracket the relative stabilities of **6** and **7**, but this issue only matters if the protonation of bromic acid is productive and, hence, there is the question as to the stability of protonated bromic acid in aqueous acidic media.

We computed the reaction energies for the protonations of bromic acid by hydronium ion leading to **6a** or **7c**, respectively. The reaction energies are highly dependent on the quality of the electron correlation treatment (especially of **5** and **7**), and they also are highly sensitive to the effects of solvation. While the reaction **5** + H_3O^+ ⇄ **6a** + H_2O is strongly exothermic in the gas phase ($\Delta E = -28.4$ kcal/mol), the stabilization of hydronium ion in aqueous solution is so overwhelming that the proton exchange reaction turns endothermic with $\Delta E^{SMD} = +7.9$ kcal/mol, a solvation effect of well over 30 kcal/mol. Accounting both for higher-level correlation and for aqueous solvation effects, the computations predict the protonation of bromic acid to be considerably endothermic ($\Delta E^{QnS} > 20$ kcal/mol) and endergonic ($\Delta G^{QnS} > 19$ kcal/mol).

The single-electron reduction of protonated bromic acid requires proximity of a protonated bromic acid molecule and the reducing agent. If the protonated species is available only as a short-lived intermediate as is indicated here, then it becomes necessary to establish proximity between bromic acid and the reducing agent *prior to* protonation, and the outcome of the protonation/reduction sequence will depend on the relative stabilities of protonated aggregates formed between bromic acid and the reducing reagent (rather than the isomer preferences of protonated bromic acid). In such a situation, the question naturally arises whether it might not be better to first reduce bromic acid prior to protonation.

(d). Reduction of Bromic Acid and Subsequent Protonation: Structure and Stability of Bromic Acid Radical Anion. We determined the structure of the bromic acid radical anion **9** at the MP2/6-311++G** and SMD(MP2/6-311++G**) levels, and the MP2 structure is shown in Figure 4 (bottom right) together with the structure of BrO_2 determined at the same level. Structure **9** is best described as a Lewis donor−acceptor complex formed between the Lewis donor hydroxide and the σ-acceptor BrO_2. In gas phase the complex formation HO^- + BrO_2 → **9** is highly exothermic with ΔE and $\Delta E'$ values of about −40 kcal/mol and also highly exergonic with ΔG and $\Delta G'$ values of about −30 kcal/mol (Table 1). In aqueous solution, however, the very strong solvation of hydroxide drastically diminishes the complex binding energy to $\Delta E = -5 \pm 2$ kcal/mol and makes complex formation endergonic with $\Delta G = +5 \pm 2$ kcal/mol (Tables 2 and 3). Hence, the dissociation of the $HO^-\cdots BrO_2$ dative bond is facile, and the dissociation of **9** with concomitant or subsequent protonation affords water and BrO_2.

(e). Synthetic Routes to $(HO)_2BrO$ Derivatives. The study of the parent radical $(HO)_2BrO$ produced two promising leads for possible synthetic exploration, and these are the addition of RO

dx.doi.org/10.1021/ic4011967 | *Inorg. Chem.* 2013, 52, 11806−11820

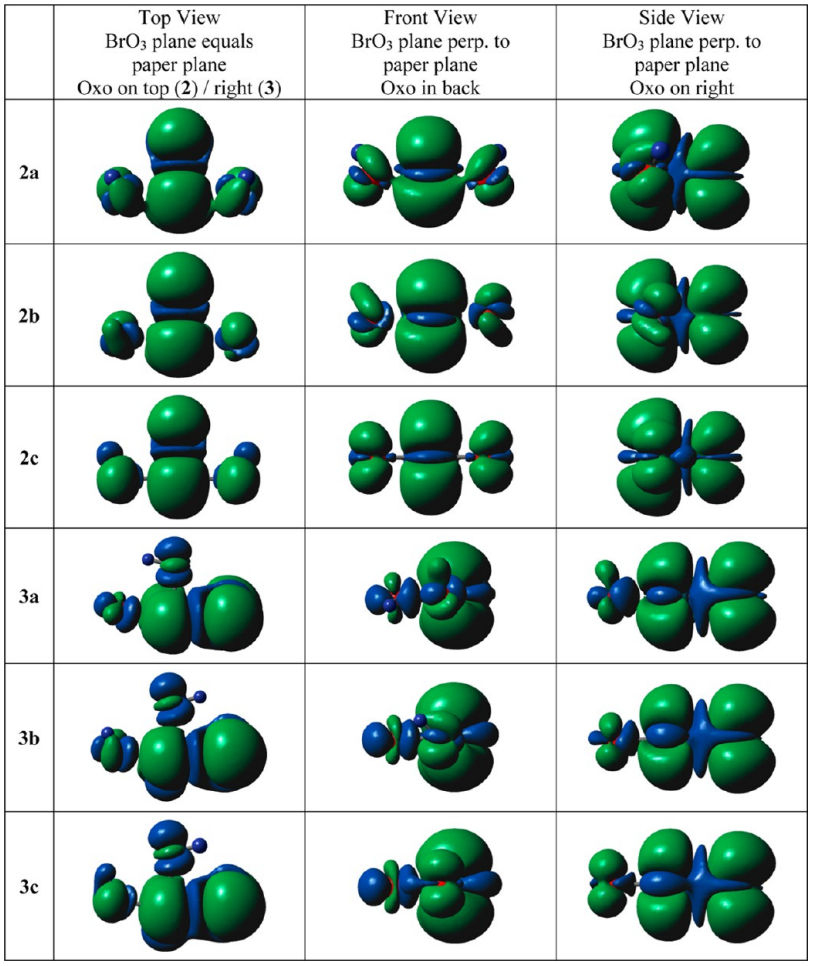

Figure 6. QCI//MP2 spin density distributions of selected stationary structures of isomers **2** and **3** of $(HO)_2BrO$ radical. Green and blue colors represent α- and β-spin density, respectively.

radical to bromous acid and bromite esters and the reduction of protonated bromic acid.

The thermochemistry of the parent reaction HOBrO + $HO^{\bullet}$ → $(HO)_2BrO$ shows the addition to be almost thermoneutral and only slightly endergonic. These results suggest that derivatives of $(HO)_2BrO$ might become accessible by addition of radicals $RO^{\bullet}$ to HOBrO, by addition of $HO^{\bullet}$ to R′OBrO esters, and/or by addition of radicals $RO^{\bullet}$ to R′OBrO esters.

It is a significant finding that isomers **6** and **7** of protonated bromic acid have similar stabilities. Strategies to prepare $(HO)_2BrO$ derivatives need to bias the system toward protonation/reduction chemistry and in favor of O-protonation (isomer **7**) over OH-protonation (isomer **6**). Variations of the medium might achieve one or both of these aims, and the employment of bromate esters should be a powerful tool to affect the regiopreference of protonation.

Electronic Structure and Molecular Orbital Analysis of $(HO)_2BrO$. A first clue toward the development of an understanding of the electronic structure of $(HO)_2BrO$ is provided by the spin density distribution. The spin density distributions computed at the QCI level for all isomers of $(HO)_2BrO$ show a 2-center-π-radical extending over the BrO moiety with only minor amounts of spin density in the OH regions (Figure 6). In Lewis structure language, one would say that both the neutral resonance form **D** and the polar resonance form **E** contribute (Scheme 5).

A second important clue is provided by the molecular ESP computed with the QCI densities (Figure 7). The ESP plots show electron deficient bromine as expected, but they do not show significant electron excess at the oxide-O and, instead, they indicate electron density excess at the hydroxyl-O's. The **D** ↔ **E** process alone cannot account for these features of the ESPs.

The third clue comes from the realization that even a maximally occupied π-system can at best delocalize one electron from bromine to the oxide-O (i.e., **E** vs. **D**), and π-delocalization *can only reduce but cannot remove* the bromine's hypervalency.

In Figure 8 are shown the occupied valence spin molecular orbitals of **2c**. A similar figure for **2a** is provided in Supporting Information, Figure S8b, and the arguments made for π-system **2c** carry over to pseudo-π-system **2a** and **2b**. The α-spin molecular orbitals (ASMO) are shown on the left in the order of decreasing orbital energy from top to bottom. The β-spin molecular orbitals (BSMO) are shown on the right, and they are not necessarily shown in the order of their energies.[60] Instead, the β-spin σ-MOs are placed next to the best shape-matching α-spin σ-MO. This mode of presentation emphasizes that it is still possible to identify pairs of α- and β-spin MOs that are very similar in shape even though spin polarization removes the spatial and energetic equality of such pairs of α-spin and β-spin MOs, and this *shape-matching is possible for all σ-SMOs* (Figure 8).

dx.doi.org/10.1021/ic4011967 | *Inorg. Chem.* 2013, 52, 11806−11820

Scheme 5. Schematic Representations of the (4c-7e) π-System of *trans*-$(HO)_2BrO$, 2c

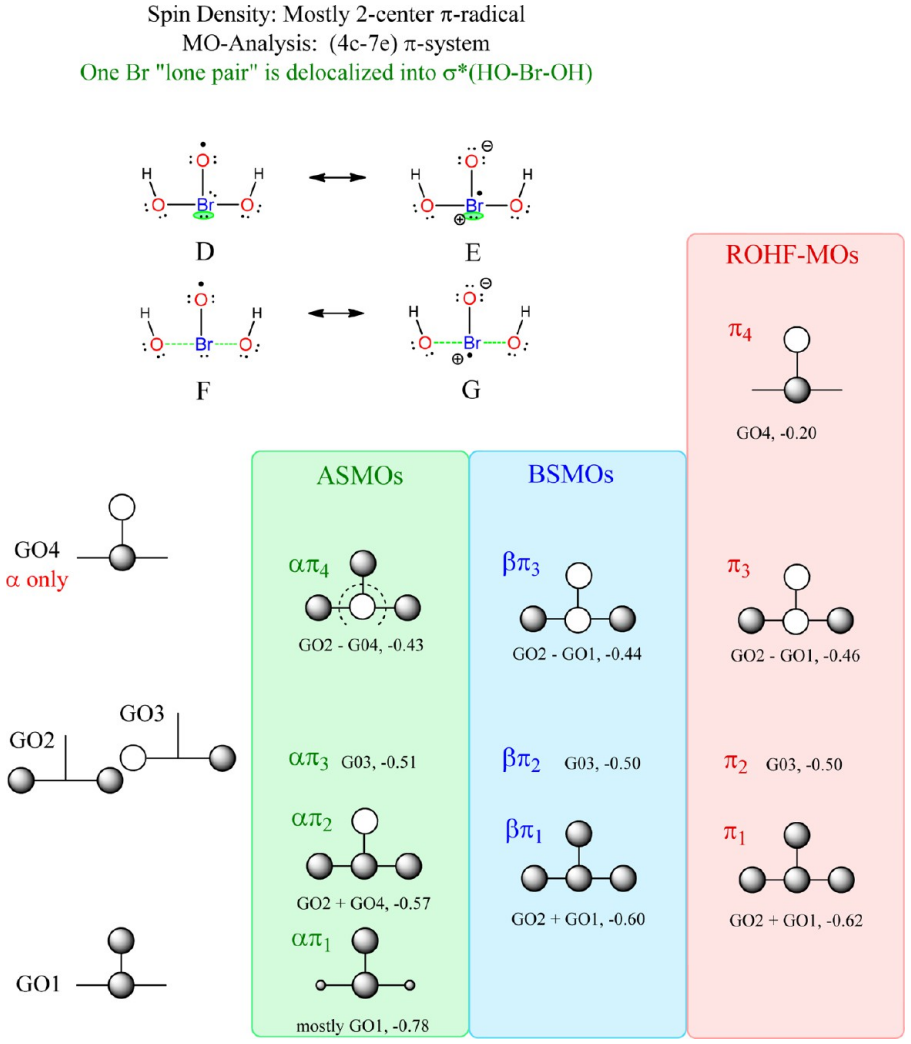

(a). Delocalization of Bromine Density into HO−Br−OH σ-MO.* In BrO_2, hypervalency is avoided because bromine contributes 3 electrons to the (3c-5e) π-system, and the remaining 4 electrons of Br are involved in 2 σ-bonds and a σ-lone pair. In $(HO)_2BrO$, bromine contributes only 2 electrons to the (4c-7e) π-system, and 5 σ-electrons remain at Br in the hypervalent Lewis structure. Three of these engage in the formation of 3 σ-bonds, and the remaining 2 σ-electrons are placed in 2 σ*-SMOs, the highest occupied spin orbitals with α- or β-spin (ASMO31 and BSMO30, shaded blue in Figure 8). The occupied σ*-SMOs can be described as antibonding linear combinations of bromine's valence s-AO and two oxygen p_{ip}-AOs.

In Scheme 5, we shaded one bromine lone pair green in **D** and **E** to indicate that these electrons are occupying σ*-SMOs. The alternative notations **F** and **G** reflect that the occupation of the σ*-SMOs reduces the Br−OH bond order to 0.5.

(b). Spin Density Distribution and (4c-7e) π-System. The most surprising feature illustrated by Figure 8 concerns the discovery that there are *five* (!) *π-SMOs with unique shapes* in the (4c-7e) π-system **2c**. Strict σ/π-separation is possible for C_{2v}-**2c**, one can easily identify four ASMOs and three BSMOs with π-symmetry, and these are highlighted in red in Figure 8. Among the 7 π-SMOs there is only one pair of α- and β-spin SMOs that are essentially of the same shape, and these are $\alpha\pi_3$ and $\beta\pi_2$. The remaining 5 π-SMOs cannot be shape-matched, not even approximately. We show the spin-orbitals $\alpha\pi_4$ and $\beta\pi_3$ and the spin-orbitals $\alpha\pi_2$ and $\beta\pi_1$ next to each other in their respective rows merely to save space in Figure 8; these 4 π-SMOs and $\alpha\pi_1$ all have different nodal properties and, therefore, they clearly are not even approximately of comparable shape. Topologically, one notes that the main difference between $\alpha\pi_2$ and $\beta\pi_1$ ($\alpha\pi_4$ and $\beta\pi_3$) is an additional node in the unique Br−O bond in the $\alpha\pi$-SMO. Considering the unique shapes of five of the π-orbitals, one has no reason to expect that any pair of them would be of comparable energy. Yet, the pairs ($\alpha\pi_2$, $\beta\pi_1$) and ($\alpha\pi_4$, $\beta\pi_3$) are nearly degenerate in spite of their definitively different shapes. Scheme 6 provides a MO level diagram of this unusual situation. Simple radicals are commonly depicted in textbooks by an MO diagram that shows one singly occupied molecular orbital (SOMO) as the highest occupied molecular orbital (HOMO). In sharp contrast, however, the HOMO of doublet radical **2c** is doubly occupied and, moreover, there are 5 unique SMOs with entirely different shapes.

The shapes of these five unique π-SMOs can be explained with group orbitals, and Scheme 5 helps to illustrate. There are four pπ-AOs, and linear combination of pairs of these generates group orbitals GO1−GO4. GO1 and GO4 are bonding and antibonding BrO group orbitals, respectively, while GO2 and GO3 are essentially nonbonding, nearly degenerate group

dx.doi.org/10.1021/ic4011967 | *Inorg. Chem.* 2013, 52, 11806−11820

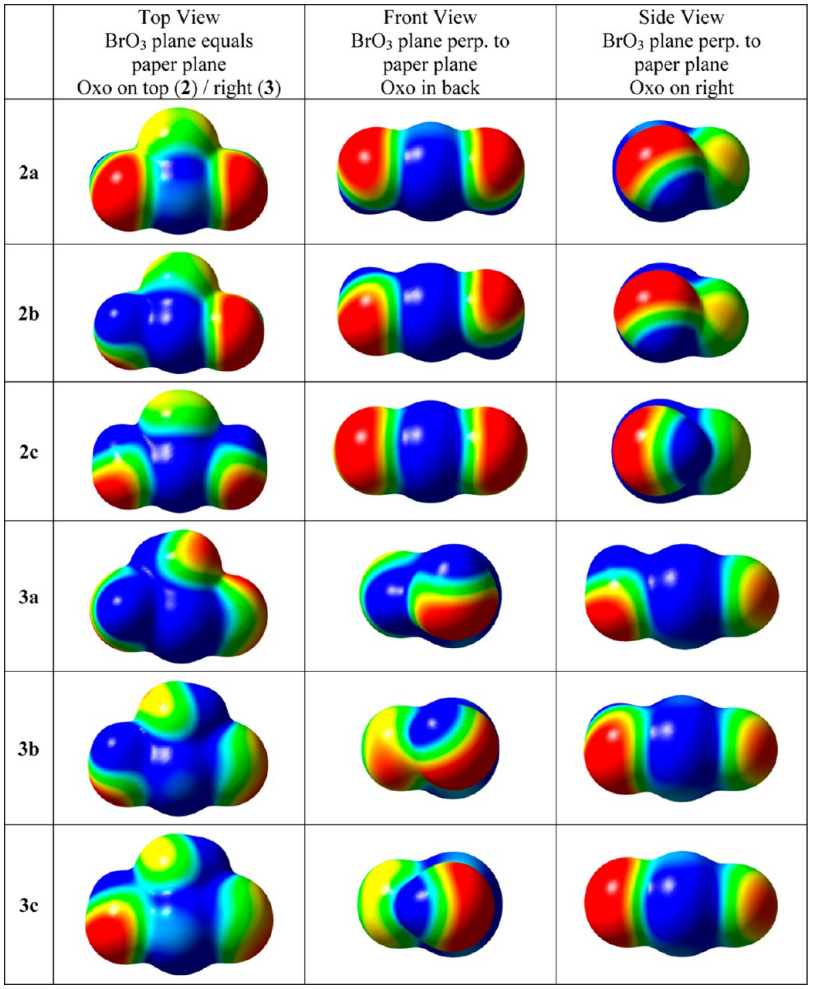

Figure 7. QCI//MP2 ESP is shown surfaced mapped on the total electron density as viewed from top, back, and side of selected stationary structures of isomers **2** and **3** of $(HO)_2BrO$ radical. Same settings were used as with BrO_2 (see Figure 2).

orbitals that correspond to lone pair electrons on hydroxyl O-atoms. There are 7 π-electrons and, hence, four occupy α-spin group orbitals (ASGO1−ASGO4) and three occupy β-spin group orbitals (BSGO1−BSGO3). Only GO3 is symmetric with regard to the C_2-axis and the α- and β-spin GO3s give rise to the one shape-matched set $\alpha\pi_3$ and $\beta\pi_2$. The other GOs all are asymmetric, and the remaining question concerns possible combinations of GO2 with GO1 and/or GO4. For the β-spin electrons, BSGO2 mixes with BSGO1 and gives rise to $\beta\pi_1$ and $\beta\pi_3$. This mode of mixing (GO1 with GO2) is the *only* option for the β-spin electrons, and it is *one* option for the α-spin electrons. If this option were realized, then one would obtain pairs of shape-matched π-SMOs and just one unique α-SMO with GO4 shape. However, Figure 8 shows that ASGO2 mixes mostly with ASGO4 to give rise to $\alpha\pi_2$ and $\alpha\pi_4$, and $\alpha\pi_1$ remains essentially ASGO1 (with very little ASGO2).

It is this freedom for the α- and β-spin electrons to occupy different linear combinations of the group orbitals that presents a fundamental difference from restricted open-shell Hartree−Fock (ROHF) theory. The π-MOs computed for the same structure C_{2v}-**2c** at the ROHF/6-311G* level are shown in 9. The mixing of GO1 with GO2 is the *only* option for the β-spin electrons, and because pairs of α- and β-spin electrons must occupy the same MOs in ROHF theory, this mixing becomes the *one and only* option for the α-spin electrons. The group orbital G04 is left as the singly occupied, highest-lying π-MO (Scheme 5, MO31 in Figure 9). The computations of C_{2v}-**2c** at the UQCISD/6-311G*//MP2/6-311G* level starting with the UHF or with the ROHF orbitals gave the exact same result. The UHF orbitals provide a more appropriate description of the radical's electronic structure than the ROHF orbitals. The characteristic spin polarization pattern of the radical is present at the UHF level and this pattern is retained in the QCI spin density distribution.

Naturally, one must wonder why ASGO2 would not mix with ASGO1 (as with the β-density) and leave the high-lying ASGO4 essentially as is. One plausible explanation invokes the optimization of spin polarization in the Br−O bond region. Irrespective as to whether ASGO2 mixed with ASGO1 or ASGO4, the (4c-7e) π-system essentially becomes a 2-center π-radical. But the choice of mixing ASGO2 either with ASGO1 or with ASGO4 greatly affects the spin density in the Br−O bond region! We pointed out above that the main difference between $\alpha\pi_2$ ($\alpha\pi_4$) and $\beta\pi_1$ ($\beta\pi_3$) is an additional node in the unique Br−O bond in the $\alpha\pi$-SMO. This additional node in $\alpha\pi_2$ ($\alpha\pi_4$) is the direct consequence of the observed mixing, and no such node would occur if ASGO2 had mixed with ASGO1 (as in the case of the ROHF orbitals). It is for the presence of this node in $\alpha\pi_2$ ($\alpha\pi_4$) that the spin density distribution of **2c** features major β-spin density in the Br−O region.

Another plausible explanation comes from the recognition that $\alpha\pi_4$ (ASGO2−ASGO4) allows for constructive overlap of the three p_π(O)-AOs in the nonbonded HO···O regions. A surface

dx.doi.org/10.1021/ic4011967 | *Inorg. Chem.* 2013, 52, 11806−11820

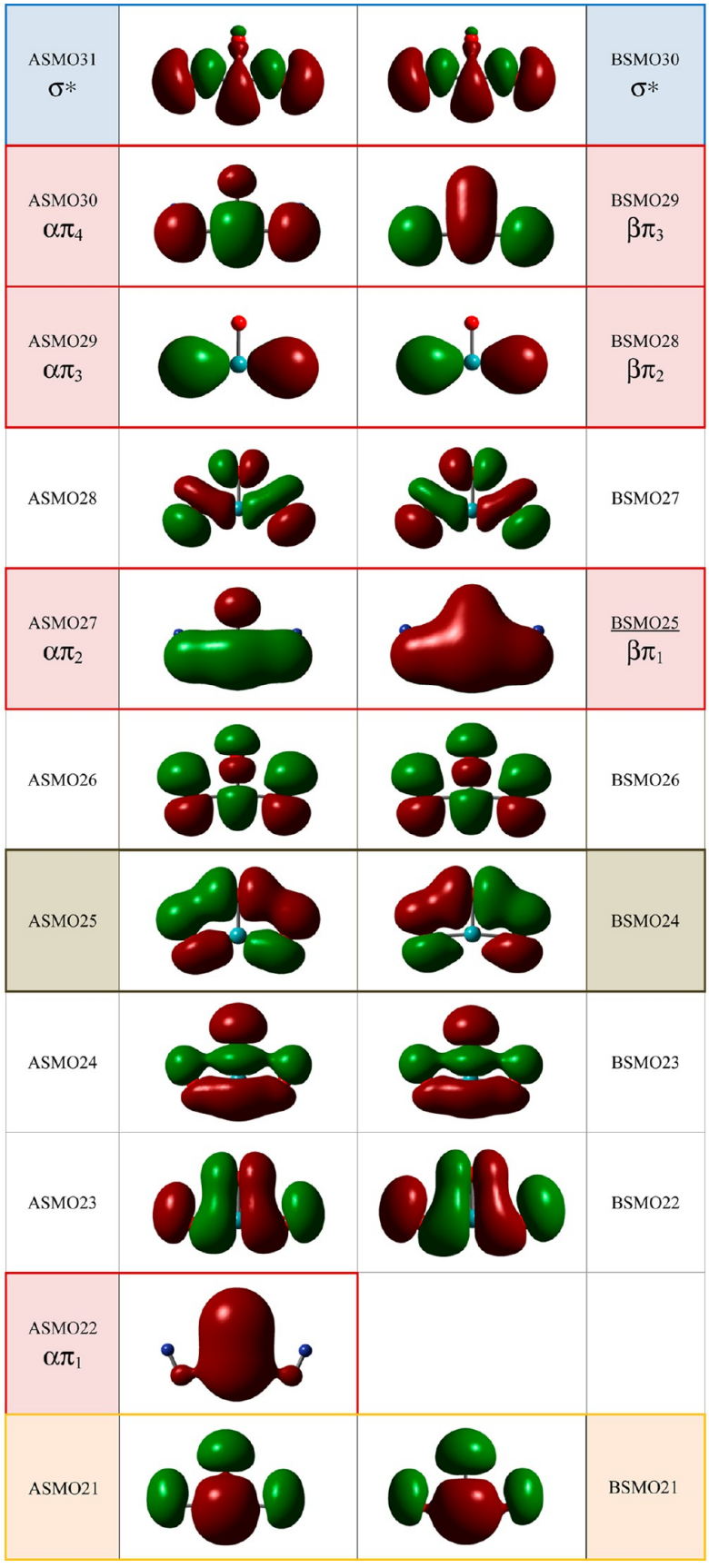

Figure 8. continued

dx.doi.org/10.1021/ic4011967 | *Inorg. Chem.* 2013, 52, 11806−11820

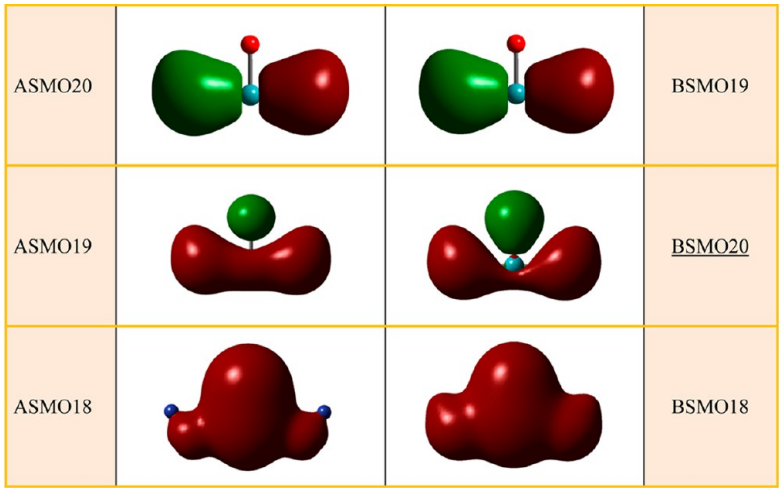

Figure 8. Spin molecular orbitals of C_{2v}-symmetric radical **2c**.

Scheme 6. MO Level Diagrams for the 27 Valence Electrons of the Doublet Radical 2c[a]

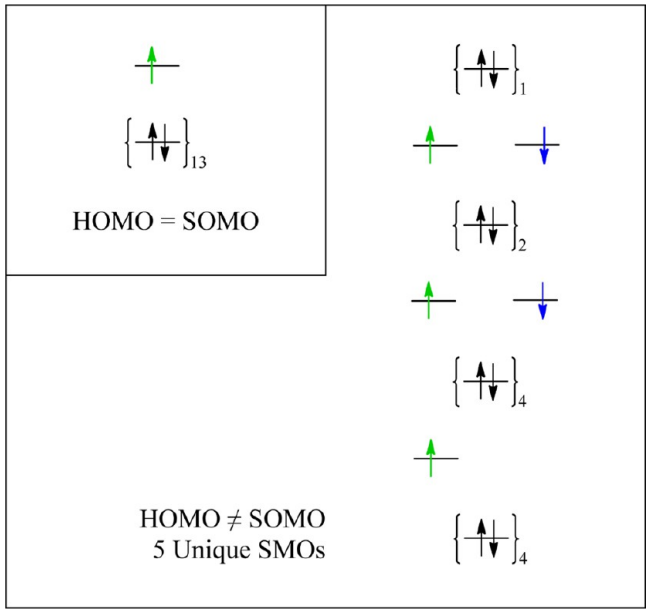

[a]Each {⇅} denotes a doubly-occupied MO (ROHF theory) or a pair of shape-matched, near-degenerate SMOs (UHF theory). The top-left panel shows the textbook situation of a simple doublet radical: the one singly-occupied MO (SOMO) also is the highest occupied MO (HOMO).

plot of $\alpha\pi_4$ with a smaller surface density value shows this overlap, and this plot is provided as Supporting Information, Figure S10.

(c). Intramolecular Hydrogen-Bonding. The spin-orbitals ASMO25 and BSMO24 are pertinent to intramolecular H-bonding, and they are highlighted in sienna in Figure 8. Four p_{ip}-AOs are combined to create SMOs which are all-bonding along the perimeter (Scheme 7). The phase relations among the p_{ip}-AOs of the O-atoms is similar to one of the e-symmetric p_{ip}-AOs in the Walsh model of cyclopropane.[9d] In contrast, however, the antibonding between two p_{ip}-AO(O) is avoided in **2c** because of the contribution from the additional p_{ip}-AO(Br). The H-atoms of **2c** are located in regions of strong overlap. These orbitals are a major reason for the conformation about the Br−OH bonds in **2c**; these advantages are retained in part in **2a** and **2b**, while they are absent in **2d**.

The orbitals ASMO26 and BSMO26 also overlap constructively in the H-bonding region, and this becomes visible when the orbitals are plotted with a lower surface density setting (Supporting Information, Figure S11).

CONCLUSIONS

The PES analysis of dihydrogen bromate $(HO)_2BrO$ shows that all stationary structures are T-shaped, that trans-dihydroxides **2** are preferred over cis-isomers **3**, and that structures with two intramolecular O−H···O bonds are preferred. The minima **2a**−**2c** are close in energy at the MP2 level with a small preference for C_{2v}-**2c** at the QCI//MP2 levels.

The study of the parent radical $(HO)_2BrO$ produced two leads for synthetic exploration. The study showed that the addition reaction HOBrO + HO$^\bullet$ → $(HO)_2BrO$ is almost thermoneutral and only slightly endergonic. Hence, derivatives of $(HO)_2BrO$ might be accessible by addition of radicals RO$^\bullet$ to HOBrO, by addition of HO$^\bullet$ to R′OBrO esters, and/or by addition of radicals RO$^\bullet$ to R′OBrO esters. It is a significant finding that the proton affinities for OH-protonation (isomer **6**) and O-protonation (isomer **7**) of bromic acid are within a few kcal/mol. Strategies to prepare $(HO)_2BrO$ derivatives therefore need to bias the system toward protonation/reduction chemistry and in favor of O-protonation (**7**) over OH-protonation (**6**). Variations of the medium and the employment of bromate esters $ROBrO_2$ might achieve one or both of these aims.

The formation of the (3c-5e) π-system causes BrO_2 to be a 3-center π-radical and suffices to avoid hypervalency in **1**. Radicals **2** and **3** also feature maximally occupied (pseudo) π-systems to transfer bromine density to the periphery, but the (4c-7e) π-systems in **2** or **3** neither manifest themselves as 4-center π-radicals nor suffice to avoid hypervalency. The electronic structures **2a**−**2c** and **3a**−**3c** are best described as heavily spin-polarized 2-center (pseudo) π-radicals centered on the bromine oxide moieties. To avoid hypervalency in $(HO)_2BrO$, bromine density is delocalized into σ*-SMOs over the trans O−Br−O moiety (HO−Br−OH in **2**, HO−Br−O in **3**) and the Br→O electron transfer manifests itself in enhanced ESPs in the oxygen regions of the trans O−Br−O moieties of **2a**−**2c** and **3a**−**3c**.

Molecular orbital theory can be employed to explain all of the electronic features. In particular, MO theory illustrates well the

dx.doi.org/10.1021/ic4011967 | *Inorg. Chem.* 2013, 52, 11806−11820

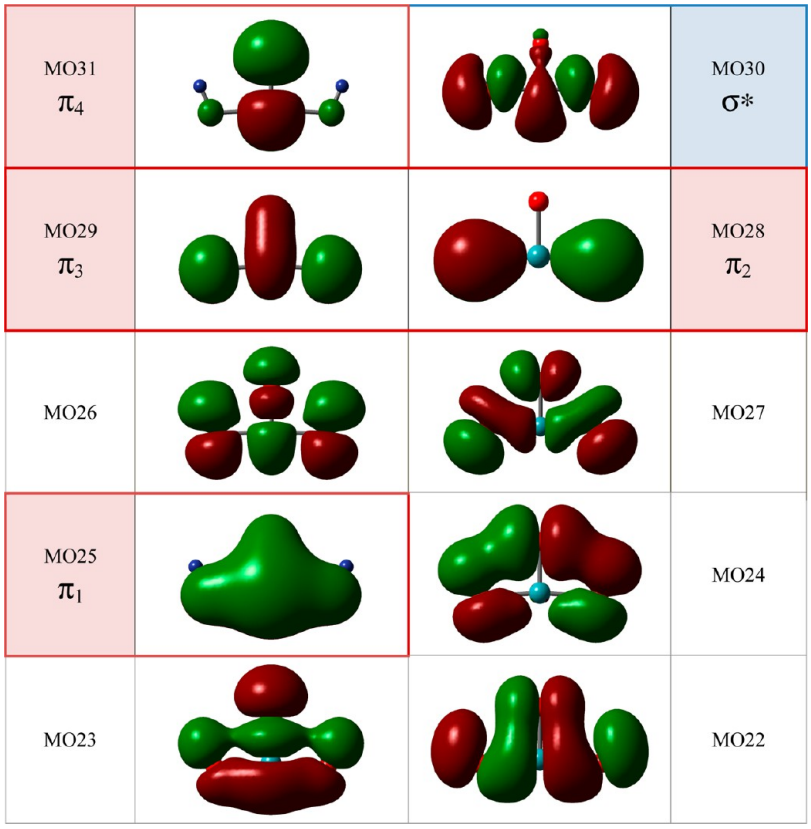

Figure 9. ROHF molecular orbitals of C_{2v}-symmetric radical **2c**. The Supporting Information includes an expanded version of this figure which shows all ROHF valence-MOs.

Scheme 7. Intramolecular H-Bonding in $(HO)_2BrO$

mechanisms for Br→O electron transfer via the (4c-7e) π-system and by population of 3-center σ^*-SMOs and the mechanisms for spin delocalization and spin polarization. The (4c-7e) π-system in C_{2v}-**2c** is remarkable in that it contains five π-symmetric spin molecular orbitals (SMO) with unique shapes, and it was shown how this feature contributes to the spin polarization of the Br−O bond. The same topological features occur in the pseudo π-systems of **2** and its isomer **3**.

■ ASSOCIATED CONTENT

Ⓢ Supporting Information

Three figures showing valence SMOs of C_2-**2a**, ROHF valence-MOs of C_2-**2c**, and selected ASMOs of C_{2v}-**2c** drawn with lower density values. One table of total energies and thermochemical parameters computed at the MP2 level and QCISD//MP2 and QCISD(T)//MP2 energies, and one table of total energies and thermochemical parameters computed at the SMD(MP2) Level. Cartesian coordinates of the MP2(full)/6-311G* and SMD-(MP2(full)/6-311G*) optimized structures of **1**, **2a**, **2c**, **4**, **5**, and **6**−**8**, and of the MP2(full)/6-311++G** and SMD(MP2(full)/6-311++G**) optimized structures of **1**, **5**, and **9**, and details of the QCISD(T)/6-311++G(2df,2pd) level computations (22 pages). This material is available free of charge via the Internet at http://pubs.acs.org

■ AUTHOR INFORMATION

Corresponding Author

*E-mail: glaserr@missouri.edu. Phone: 573-882-0331.

Notes

The authors declare no competing financial interest.

■ ACKNOWLEDGMENTS

This research was supported in part by NSF-PRISM grant *Mathematics and Life Sciences* (#0928053). The ab initio computations were performed with the HPC resources of the University of Missouri Bioinformatics Consortium (UMBC).

■ REFERENCES

(1) Musher, J. I. *Angew. Chem., Int. Ed.* **1969**, *8*, 54−68.
(2) Jensen, W. *J. Chem. Educ.* **2006**, *83*, 1751−1752.
(3) (a) Rundle, R. E. *J. Am. Chem. Soc.* **1947**, *69*, 1327−1331. (b) Pimentel, G. *J. Chem. Phys.* **1951**, *19*, 446−448.
(4) Noury, S.; Silvi, B.; Gillespie, R. J. *Inorg. Chem.* **2002**, *41*, 2164−2172.
(5) Kalemos, A.; Mavridis, A. *J. Phys. Chem. A* **2011**, *115*, 2378−2384.
(6) Sajith, P. K.; Suresh, C. H. *Inorg. Chem.* **2012**, *51*, 967−977.
(7) Schmøkel, M. S.; Cenedese, S.; Overgaard, J.; Jørgensen, M. R. V.; Chen, Y.; Gatti, C.; Stalke, D.; Iversen, B. B. *Inorg. Chem.* **2012**, *51*, 8607−8616.
(8) (a) IUPAC. Compendium of Chemical Terminology, 2nd ed. (the "Gold Book"). McNaught, A. D., Wilkinson, A., Eds.; Blackwell Scientific Publications: Oxford, U.K., 1997. (b) XML on-line corrected version: http://goldbook.iupac.org (2006-) created byNic, M.; Jirat, J.; Kosata, B.; updates compiled by Jenkins, A. Last update: 2012-03-23; version: 2.3.1. DOI: 10.1351/goldbook.HT07054. (c) IUPAC defines "hypervalency" as the "ability of an atom in a molecular entity to expand its valence shell beyond the limits of the Lewis octet rule. Hypervalent

compounds are common for the second and subsequent row elements in groups 15−18 of the periodic table. A description of the hypervalent bonding implies a transfer of the electrons from the central (hypervalent) atom to the nonbonding molecular orbitals which it forms with (usually more electronegative) ligands. A typical example of the hypervalent bond is a linear three-centre, four-electron bond, e.g. that of $F_{ap}-P-F_{ap}$ fragment of PF_5."

(9) (a) Burdett, J. K.; Whangbo, M.-H. *Orbital Interactions in Chemistry*; John Wiley & Sons: New York, 1985. (b) 258ff. (c) 12ff. (d) 184ff.

(10) Curnow, O. J. *J. Chem. Educ.* **1998**, *75*, 910.

(11) (a) Landis, C. R.; Firman, T. K.; Root, D. M.; Cleveland, T. *J. Am. Chem. Soc.* **1998**, *120*, 1842−1854. (b) Cleveland, T.; Landis, C. R. *J. Am. Chem. Soc.* **1996**, *118*, 6020−6030.

(12) Woon, D. E.; Dunning, T. H. *J. Phys. Chem. A* **2009**, *113*, 7915−7926.

(13) (a) Braïda, B.; Hiberty, P. C. *J. Am. Chem. Soc.* **2004**, *126*, 14890−14898. (b) Braïda, B.; Hiberty, P. C. *J. Phys. Chem. A* **2008**, *112*, 13045−13052.

(14) Magnusson, E. *J. Am. Chem. Soc.* **1990**, *112*, 7940−7951.

(15) Wang, P.; Zhang, Y.; Glaser, R.; Reed, A.; Schleyer, P. v. R.; Streitwieser, A. *J. Am. Chem. Soc.* **1991**, *113*, 55−64.

(16) (a) Smith, D. W. *J. Chem. Educ.* **2005**, *82*, 1202−1204. (b) Schleyer, P. v. R. *Chem. Eng. News* **1984**, *62*, 4.

(17) Chu, S.-Y.; Lee, S.-L. *J. Chem. Educ.* **1985**, *62*, 857−858.

(18) Landis, C. R.; Weinhold, F. *J. Chem. Educ.* **2012**, *89*, 570−572.

(19) Berg, S.; Ghosh, A. *J. Chem. Educ.* **2011**, *88*, 1663−1666.

(20) Glaser, R.; Jost, M. *J. Phys. Chem. A* **2012**, *116*, 8352−8365.

(21) Farooq, U.; Shah, A. A.; Wirth, T. *Angew. Chem., Int. Ed.* **2009**, *48*, 1018−1020.

(22) Ochiai, M. *Synlett* **2009**, 159−173.

(23) (a) Fu, H.; Xie, S.; Fu, A.; Lin, X.; Zhao, H.; Ye, T. *Org. Biomol. Chem.* **2012**, *10*, 6333−6340. (b) Ochiai, M.; Yoshimura, A.; Miyamoto, K.; Hayashi, S.; Nakanishi, W. *J. Am. Chem. Soc.* **2010**, *132*, 9236−9239.

(24) Ochiai, M.; Yoshimura, A.; Hoque, M. M.; Okubo, T.; Saito, M.; Miyamoto, K. *Org. Lett.* **2011**, *13*, 5568−5571.

(25) Cramer, C. J. *Essentials of Computational Chemistry*; Wiley: New York, 2004.

(26) Pople, J. A. *Rev. Modern Phys.* **1999**, *71*, 1267−1274.

(27) Wilson, S. *Handb. Mol. Phys. Quantum Chem.* **2003**, *2*, 314−373.

(28) (a) Krishnan, R.; Binkley, J. S.; Seeger, R.; Pople, J. A. *J. Chem. Phys.* **1980**, *72*, 650−654. (b) Curtiss, L. A.; Binning, R. C., Jr. *Int. J. Quantum Chem.* **1991**, *40*, 781−787.

(29) Shavitt, I.; Bartlett, R. J. *Many-Body Methods in Chemistry and Physics: MBPT and Coupled-Cluster Theory*; Cambridge University Press: Cambridge, U.K., 2009.

(30) (a) Pople, J. A.; Head-Gordon, M.; Raghavachari, K. *J. Chem. Phys.* **1987**, *87*, 5968−5975. (b) Pople, J. A. *Nobel Lecture: Quantum Chemical Models. Rev. Mod. Phys.* **1999**, *71*, 1267−1274.

(31) Frisch, M. J.; Pople, J. A.; Binkley, J. S. J. *Chem. Phys.* **1984**, *80*, 3265−3269.

(32) (a) Ribeiro, R. F.; Marenich, A. V.; Cramer, C. J.; Truhlar, D. G. *J. Comput.-Aided Mater.* **2010**, *24*, 317−333. (b) Marenich, A. V.; Cramer, C. J.; Truhlar, D. G. *J. Phys. Chem. B* **2009**, *113*, 6378−6396.

(33) (a) Marenich, A. V.; Cramer, C. J.; Truhlar, D. G. *J. Phys. Chem. B* **2009**, *113*, 4538−4543. (b) Halim, M. A.; Shaw, D. M.; Poirier, R. A. *THEOCHEM* **2010**, *960*, 63−72. (c) Saielli, G. *J. Phys. Chem. A* **2010**, *114*, 7261−7265.

(34) Frisch, M. J.; Trucks, G. W.; Schlegel, H. B.; Scuseria, G. E.; Robb, M. A.; Cheeseman, J. R.; Scalmani, G.; Barone, V.; Mennucci, B.; Petersson, G. A.; et al. *Gaussian 09*, Rev. A.1; Gaussian, Inc.: Wallingford, CT, 2009.

(35) Dennington, R.; Keith, T.; Millam, J. *GaussView* 5.0.8; Semichem Inc.: Shawnee Mission, KS, 2009.

(36) (a) Murray, J. S., Sen, K., Eds.; *Molecular Electrostatic Potentials, Vol. 3: Concepts and Applications (Theoretical and Computational Chemistry)*. Elsevier Science: New York, 1996. (b) Politzer, P.; Truhlar, D. G. *Chemical Applications of Atomic and Molecular Electrostatic Potentials: Reactivity, Structure, Scattering, and Energetics of Organic, Inorganic, and Biological Systems*; Springer: New York, 1981.

(37) (a) Magnasco, V. *Elementary Methods of Molecular Quantum Mechanics*; Elsevier Science: Amsterdam, The Netherlands, 2006; p 215ff. (b) Ruiz, E.; Cirera, J.; Alvarez, S. *Coord. Chem. Rev.* **2005**, *249*, 2649−2660.

(38) Diercksen, G. H. F.; Sadlej, A. J. *J. Chem. Phys.* **1981**, *75*, 1253−1266.

(39) Handy, N. C.; Schaefer, H. F. *J. Chem. Phys.* **1984**, *81*, 5031−5333.

(40) Wiberg, K. B.; Hadad, C. M.; LePage, T. L.; Breneman, C. M.; Frisch, M. J. *J. Phys. Chem.* **1992**, *96*, 671−679.

(41) (a) Försterling, H. D.; Lamberz, H. J.; Schreiber, H. *Z. Naturforsch.* **1980**, *35a*, 1354. (b) Buxton, G. V.; Dainton, F. S. *Proc. R. Soc. London, Ser. A* **1968**, *304*, 427.

(42) Alves, W. A.; Cortes, C. E. S.; Faria, R. B. *Inorg. Chem.* **2004**, *43*, 4112−4114.

(43) Sastry, D. L.; Rao, K. V. S. R. *J. Chem. Phys.* **1985**, *82*, 639−644.

(44) Zuo, Z.; Katsumura, Y. *Faraday Trans.* **1998**, *94*, 3577−3580.

(45) Francisco, J. S. *Chem. Phys. Lett.* **1998**, *288*, 307−310.

(46) Wang, Y.; Fu, X.-Y.; Liu, R.-Z.; Xie, Y.; Schaefer, H. F. *Mol. Phys.* **2000**, *98*, 879−890.

(47) Müller, H. S. P.; Miller, C. E.; Cohen, E. A. *Angew. Chem., Int. Ed. Engl.* **1996**, *35*, 2129−2131.

(48) Miller, C. E.; Nickolaisen, S. L.; Francisco, J. S.; Sander, S. P. *J. Chem. Phys.* **1997**, *107*, 2300−2307.

(49) Wen, H.; Hou, G.-L.; Huang, W.; Govind, N.; Wang, X.-B. *J. Chem. Phys.* **2011**, *135*, 184309/1−184309/11.

(50) Byberg, J. R. *J. Chem. Phys.* **1986**, *85*, 4790−4793.

(51) Vetter, R.; Ritschel, T.; Zülicke, L. *J. Phys. Chem. A* **2003**, *107*, 2405−1412.

(52) Pacios, L. F.; Gómez, P. C. *J. Mol. Struct.: THEOCHEM* **1999**, *467*, 223−231.

(53) Kahn, S. D.; Hehre, W. J.; Pople, J. A. *J. Am. Chem. Soc.* **1987**, *109*, 1871−1873.

(54) (a) Glaser, R.; Choy, G. S.-C.; Chen, G. S.; Grützmacher, H. *J. Am. Chem. Soc.* **1996**, *118*, 11617−11628. (b) Glaser, R.; Choy, G. S.-C. *J. Phys. Chem.* **1994**, *98*, 11379−11393. (c) Glaser, R.; Choy, G. S.-C. *J. Phys. Chem.* **1993**, *97*, 3188−3198.

(55) (a) Glaser, R.; Sui, Y.; Sarkar, U.; Gates, K. *J. Phys. Chem. A* **2008**, *112*, 4800−4814. (b) Sui, Y.; Glaser, R.; Sarkar, U.; Gates, K. *J. Chem. Theory Comput.* **2007**, *3*, 1091−1099.

(56) (a) Yin, J.; Glaser, R.; Gates, K. S. *Chem. Res. Toxicol.* **2012**, *25*, 620−633. (b) Yin, J.; Glaser, R.; Gates, K. S. *Chem. Res. Toxicol.* **2012**, *25*, 634−645.

(57) Glaser, R.; Prugger, K. *J. Agric. Food Chem.* **2012**, *60*, 1776−1787.

(58) (a) Shukla, S. N.; Taqi, S. *Oxid. Commun.* **1989**, *12*, 9−14. (b) Char, P. N.; Sondu, S.; Sethuram, B.; Rao, T. N. *Indian J. Chem.* **1987**, *26A*, 749−751. (c) Ayoko, G. A.; Iyun, J. F.; El-Idris, I. F. *Trans. Metal Chem.* **1991**, *16*, 145−148.

(59) IUPAC. Compendium of Chemical Terminology, 2nd ed. (the "Gold Book"). Compiled by McNaught, A. D.; and Wilkinson, A.. Blackwell Scientific Publications, Oxford (1997). XML on-line corrected version: http://goldbook.iupac.org (2006-) created by Nic, M.; Jirat, J.; Kosata, B.; updates compiled by Jenkins, A.. ISBN 0−9678550−9-8. doi:10.1351/goldbook.

(60) The shapes of the 8 lowest-lying valence-MOs (orange in Figure 8) are readily understood as LCAOs of mostly s-type AOs on all atoms while ASMO20 and BSMO19 also include contributions from a bromine p_{ip}-AO. Among these, BSMO20 is placed below BSMO19 because BSMO20 most closely matches the shape of ASMO19 while BSMO19 most closely matches ASMO20.